Kobe University Repository : Kernel

PDF issue: 2025-12-05

Phase transitions and crystal structures of organometallic ionic plastic crystals comprised of ferrocenium cations and CH2BrBF3 anions

Kimata, Hironori

Mochida, Tomoyuki

(Citation)
Journal of Organometallic Chemistry,895:23-27

(Issue Date)
2019-09-01

(Resource Type)
journal article

(Version)
Accepted Manuscript

(Rights)
© 2019 Elsevier B.V.
This manuscript version is made available under the CC-BY-NC-ND 4.0 license
http://creativecommons.org/licenses/by-nc-nd/4.0/

(URL)
https://hdl.handle.net/20.500.14094/90006154

KOBE UNIVERSITY

Phase transitions and crystal structures of organometallic ionic plastic crystals comprised of ferrocenium cations and CH_2BrBF_3 anions

Hironori Kimata, Tomoyuki Mochida*

Department of Chemistry, Graduate School of Science, Kobe University, Rokkodai, Nada, Kobe, Hyogo 657-8501, Japan

*Corresponding author.

E-mail address: tmochida@platinum.kobe-u.ac.jp (T. Mochida)

ABSTRACT

Salts of cationic sandwich complexes often exhibit a phase transition to an ionic plastic phase at high temperature. In this study, we synthesized the salts $[Fe(C_5Me_5)_2][CH_2BrBF_3]$ (**1**), $[Fe(C_5Me_4H)_2][CH_2BrBF_3]$ (**2**), and $[Fe(C_5H_5)_2][CH_2BrBF_3]$ (**3**) containing the CH_2BrBF_3 anion in order to investigate the effect of anion symmetry. These salts underwent phase transitions to a plastic phase at 360.8, 269.9, and 328.8 K; only **2** exhibited a plastic phase below 300 K. Moreover, the crystal structures of the plastic phases and low temperature phases were investigated. The results were discussed and compared with the corresponding CF_3BF_3 salts.

Keywords: ionic plastic crystals · sandwich complexes · phase transitions · crystal structures · thermal properties

1. Introduction

Recently, organic ionic plastic crystals containing onium cations have attracted significant attention owing to their high ionic conductivities, which is advantageous for use as electrolytes and for other applications [1]. In the plastic phase, the center of gravity of each molecule is ordered, whereas the molecular orientation is disordered due to their rapid rotation [2]. Salts of cationic sandwich complexes also exhibit plastic phases, but their transition temperatures (T_C) to the plastic phase are very high (~300–500 K) [3-5], rendering them less suitable for electrochemical applications and physical measurements compared to onium salts. To lower the phase transition temperature by molecular design, we studied the correlation between the phase transition temperatures and molecular volumes and shape [4-6], and found that the $CF_3BF_3^-$ is a useful anion that produce salts with transition temperatures below 300 K (e.g. $[FeCp_2][CF_3BF_3]$: T_C = 270 K; Cp = C_5H_5) [7]. Plastic crystals containing ferrocenium cations are also interesting in terms of magnetic ionic plastic crystals [8].

In this context, we examined the effects of anion symmetry on the phase transition. Ferrocenium salts with $CH_2BrBF_3^-$ (V = 88 Å^3; Fig. 1b, left) were synthesized with a similar volume and shape to that of $CF_3BF_3^-$ (V = 84 Å^3; Fig. 1b, right), but less symmetric. This paper reports the phase transitions and crystal structures of $[FeCp^*_2][CH_2BrBF_3]$ (**1**), $[Fe(C_5Me_4H)_2][CH_2BrBF_3]$ (**2**), and $[FeCp_2][CH_2BrBF_3]$ (**3**) (Cp* = C_5Me_5; Fig. 1). In addition, the magnetic susceptibility of **2**, with a transition temperature below 300 K, was investigated.

a)

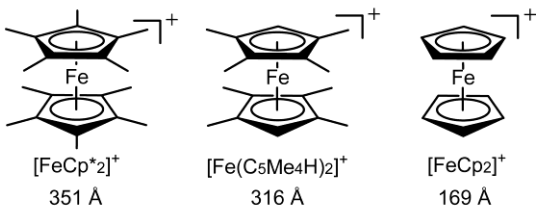

b)

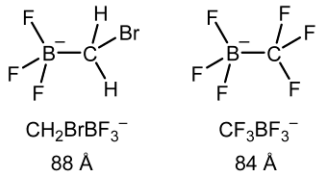

Fig. 1. Structural formula of the (a) the cationic sandwich complexes used in this study and (b) the CH_2BrBF_3 and CF_3BF_3 anions. The van-der-Waals volumes of the molecules, as estimated by DFT calculations, are shown below each formula.

2. Results and discussion

2.1. Thermal properties

Thermal properties of **1**–**3** were investigated by differential scanning calorimetry (DSC). The phase sequences and DSC traces of the prepared compounds are shown in Fig. 2a and Fig. S1 (Supplementary material), respectively. Salts **1**, **2**, and **3** exhibited a phase transition to the plastic phase (phase I) at 360.8 K (ΔS = 40.1 J mol^{-1} K^{-1}), 269.9 K (ΔS = 29.0 J mol^{-1} K^{-1}), and 328.8 K (ΔS = 41.5 J mol^{-1} K), respectively. Therefore, only **2** exhibits a plastic phase at below 300 K. Phase transition to the plastic phase was also confirmed by polarized optical microscopy with the loss of birefringence.

Interestingly, **1** exhibited a metastable phase that exhibits a lower transition temperature to the plastic phase. The entire phase sequence is shown in Fig. 3. Upon heating, phase III undergoes a transition to phase II (stable phase) at 202.7 K, followed by transition to the plastic phase (phase I) at 360.8 K (ΔS = 40.1 J mol^{-1} K^{-1}). Upon cooling the plastic phase, a transition to phase IV (the metastable phase) occurred, and when heated, this phase transitioned to the plastic phase at 334.1 K (ΔS = 9.2 J mol^{-1} K^{-1}). This transition temperature was lower than that of phase II by approximately 10 °C. This is ascribed to higher disorder of phase IV compared to that of phase II, as can be seen from their transition entropies to the plastic phase (9.2 vs. 40.19 J mol^{-1} K^{-1}). Upon cooling of phase IV, a transition to phase II occurred at 273.1 K.

The phase sequences of the prepared salts were different from those of the corresponding CF_3BF_3 salts (Fig. 2b [7]), though some similarities were observed. In both series, the transition temperature of the octamethylferrocenium salt was lower than that of the decamethylferrocenium salt, as was observed in salts with other anions [4]. The phase transition temperatures of the

octamethylferrocenium salts were comparable at approximately 270 K, but unlike the CF_3BF_3 salt that exhibited an unusually broad phase transition, the CH_2BrBF_3 salt exhibited a sharp, normal phase transition. Variations in the transition temperatures and phase sequences between the CH_2BrBF_3 and CF_3BF_3 salts suggests large structural differences between the respective compounds.

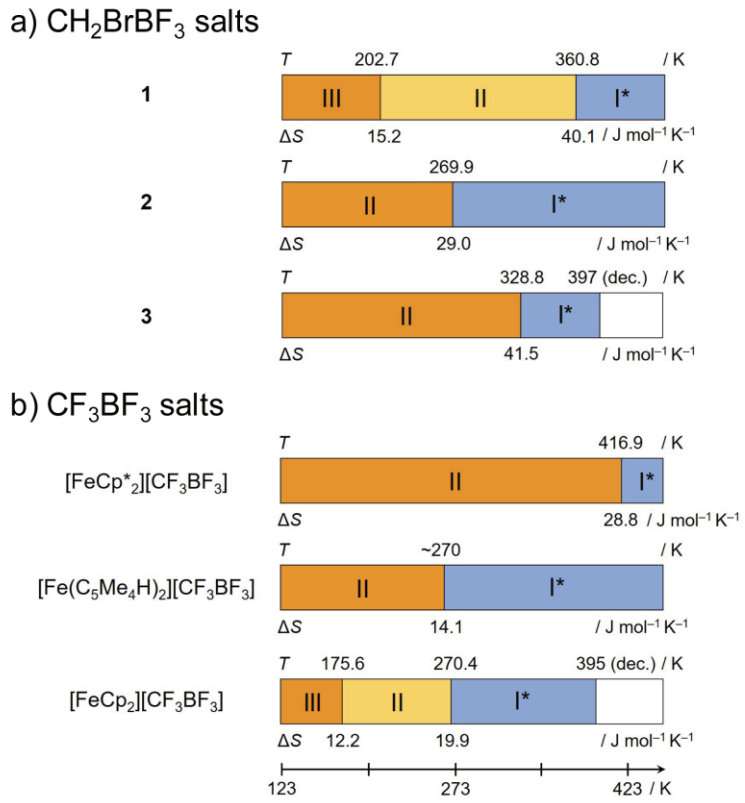

Fig. 2. Phase sequences of the (a) CH_2BrBF_3 and (b) CF_3BF_3 salts [7]. The phase transition temperatures (K) and transition entropies (J mol^{-1} K^{-1}) are shown above and below the bar charts, respectively. Asterisks indicate the plastic phases.

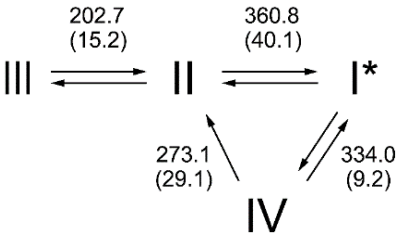

Fig. 3. Phase diagram of **1**. Phase transition temperatures (K) and transition entropies (J mol^{-1} K^{-1}, in parenthesis) are also provided.

*2.2. Low temperature structures of **1** and **3***

The crystal structures of **1** in the room-temperature phase (Phase II, 223 K) and **3** in the low-temperature phase (Phase II, 100 K) were determined. The packing diagrams of the salts are shown in Fig. 4 and the ORTEP diagrams are shown in Fig. S2 (Supplementary material). The anion exhibited no disorder in both salts.

Salt **1** crystallized in the space group $P\bar{1}$ (Fig. 4a). A pair of cation and anion was crystallographically independent, and the cations and anions were arranged nearly alternatingly. The cations have mutual contacts and each cation is surrounded by seven anions. The C_5 axes of the ferrocenes were aligned along the same direction in the crystal, providing the structure with uniaxial magnetic anisotropy. This tendency has been observed in a number of deca- and octamethylferrocenium salts [4,5]. The structural features of **1** contrast with those of the corresponding CF_3BF_3 salt $[FeCp^*_2][CF_3BF_3]$ [7]. $[FeCp^*_2][CF_3BF_3]$ exhibited higher crystal symmetry (space group: *Pnnm*) with a regular alternating cation-anion arrangement and the CF_3BF_3 anion exhibited disorder, leading to isotropic cation-anion electrostatic interactions. The low symmetry of the structure of **1** compared to that of the CF_3BF_3 salt is a consequence of the lower symmetry of the anion, which is likely responsible for the large difference in the thermal properties between the CH_2BrBF_3 and CF_3BF_3 salts. The crystal structure in phase III could not be determined due to crystal degradation.

Salt **3** crystallized in the space group *Pmmn* (Fig. 4b). The three cations and two anions were crystallographically independent and the molecule containing Fe2 exhibited a two-fold rotational disorder of its Cp rings. The anion and cation were alternately arranged and eight anions surrounded one cation. The C_5 axes of the cation in the unit cell were directed in three directions, forming a structure without magnetic anisotropy.

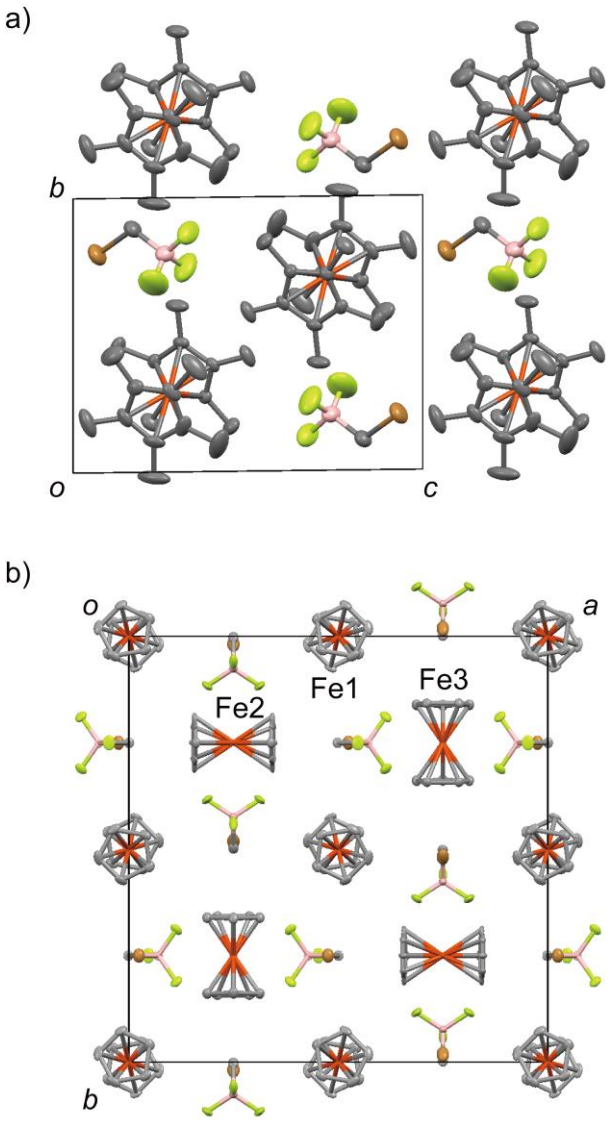

Fig. 4. Packing diagrams of (a) $[FeCp^*_2][CH_2BrBF_3]$ (**1**) at 223 K and (b) $[FeCp_2][CH_2BrBF_3]$ (**3**) at 100 K. The hydrogen atoms were omitted for clarity.

2.3. Structure of the plastic phase

The powder X-ray diffraction patterns of **1**–**3** in the plastic phase are shown in Fig. 5. Analysis of these patterns revealed that **1** and **2** adopted an *anti*-NiAs-type structure, whereas **3** adopted a CsCl-type structure. A few organic ionic plastic salts exhibit an *anti*-NiAs-type structure [1c], whereas $[Fe(C_5Me_4H)_2]X$ (X = $B(CN)_4$, $C(CN)_3$, CF_3BF_3 [5,7]) adopted this structure in the plastic phase. The lattice constants and interionic distances determined from the analysis are shown in Table 1. The van-der-Waals radii of the cations in **1**, **2**, and **3** estimated from DFT calculations were 4.37, 4.22, and

3.43 Å [6], respectively, whereas that for $[CH_2BrBF_3]^-$ was 2.76 Å. The interionic distances determined via powder X-ray diffraction experiments were almost the same as the sum of the calculated radii. The radius ratio rule generally applies to inorganic ionic crystals and predicts a coordination number of six for a structure with $0.41 < \rho < 0.73$ and a coordination number of eight for a structure with $0.73 < \rho$, where the radius ratio (ρ) is the ratio of the radius of the smaller ion to that of larger ion [9]. The radius ratios for **1**, **2**, and **3** were 0.63, 0.65, and 0.80, respectively, and they were consistent with the coordination numbers in the plastic phase.

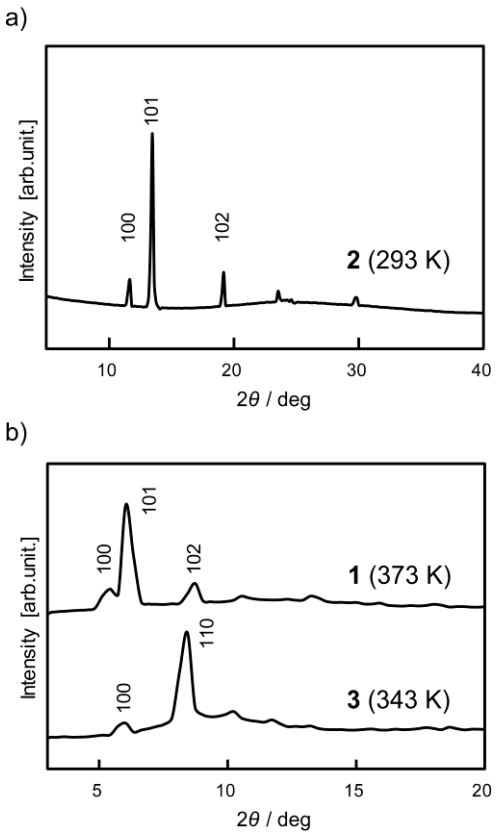

Fig. 5. Powder X-ray diffraction patters of (a) $[Fe(C_5Me_4H)_2][CH_2BrBF_3]$ (**2**) (CuKα radiation) at 293 K, and (b) $[FeCp^*_2][CH_2BrBF_3]$ (**1**) at 373 K and $[FeCp_2][CH_2BrBF_3]$ (**3**) at 343 K (MoKα radiation).

Table 1. Structure types, lattice constants, interionic distances, and radius ratios of **1**–**3**.

Salt	Temperature (K)	Structure type	lattice constants (Å)	interionic distances (Å)		radius ratio [a]
				Exp.	Calc.[a]	
1	373	*anti*-NiAs	$a = b = 8.68$, $c = 15.56$	7.21	7.13	0.63
2	293	*anti*-NiAs	$a = b = 8.73$, $c = 13.17$	6.69	6.98	0.65
3	343	CsCl	$a = b = c = 6.85$	5.93	6.19	0.80

[a]Based on the van-der-Waals volume estimated by DFT calculations.

*2.4. Magnetic susceptibility of **2***

Salt **2** exhibited a phase transition to the plastic phase below 300 K. Therefore, the temperature dependence of its magnetic susceptibility was measured to determine the susceptibility change at the phase transition (Fig. 6). Salt **2** was a paramagnetic ionic plastic crystal, exhibiting simple paramagnetic behavior down to low temperatures. The χT value at 250 K was 0.69 emu K mol^{-1}, which is reasonable for a ferrocenium salt [10]. A very slight change in magnetic susceptibility (0.01 emu K mol^{-1}) was observed at the phase transition to the plastic phase (T_C = 270 K), similar to those of other salts exhibiting a transition to the plastic phase [7]. The decrease of the magnetic susceptibility at the phase transition upon cooling from the plastic phase indicates the absence of magnetic field orientation effect, which can be ascribed to small structural magnetic anisotropy. Thus, we have not observed a magnetic field orientation effect in paramagnetic plastic crystals to date, though electric field orientation in plastic crystals [11] and magnetic field orientation in magnetic ionic liquids is certainly possible [12].

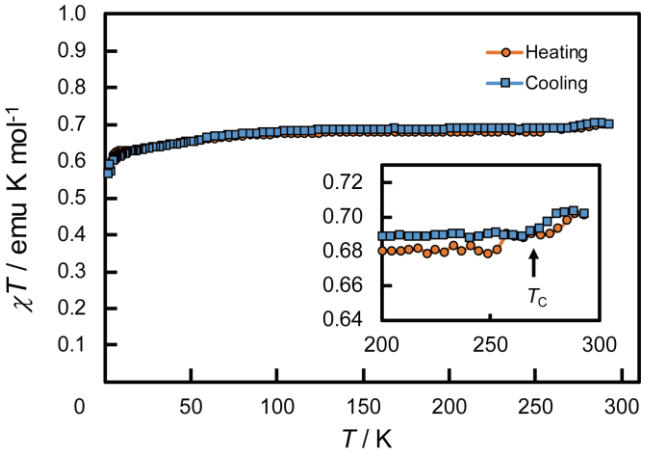

Fig. 6. Temperature dependence of the magnetic susceptibility (χT–T plots) of $[Fe(C_5Me_4H)_2][CH_2BrBF_3]$ (**2**) measured under 1 T. The cooling and heating data are indicated by

open and filled symbols, respectively. The inset shows a magnified view around the phase transition temperature.

3. Conclusion

We synthesized ferrocenium salts containing the CH_2BrBF_3 anion and investigated their phase transition to the plastic phase. The octamethylferrocenium salt exhibited a transition to the plastic phase below 300 K, whereas the transitions of the other samples were observed at higher temperatures. Only a few metallocenium salts exhibit a transition to the plastic phase below 300 K, hence this anion was found to be useful to produce salts with low transition temperatures, similar to that of the CF_3BF_3 anion. However, the phase behaviors and transition temperatures of CH_2BrBF_3 salts differed significantly from those of the CF_3BF_3 salts, despite having a similar anion size and shape. This can be ascribed to the lower symmetry of the anion, leading to different crystal structures. The octamethylferrocenium salt was a paramagnetic ionic plastic crystal at room temperature, whereas it exhibited only slight magnetic susceptibility changes at the phase transition.

4. Experimental

4.1. General

$[FeCp_2]Cl$ was prepared according to a previously described method [13]. Other chemicals were obtained commercially. DSC measurements were performed using a TA Instruments Q100 differential scanning calorimeter at a rate of 10 K min^{-1}. The decomposition temperatures were determined based on visual inspection with a microscope equipped with a heating stage. The infrared spectra were recorded via attenuated total reflectance (diamond ATR) using a Thermo Scientific Nicolet iS-5 FT-IR spectrometer. Magnetic susceptibilities were measured using a Quantum Design MPMS-XL instrument under a 1 T magnetic field. The powder XRD measurements were performed using a Rigaku SmartLab. The van der Waals volumes of the molecular ions were estimated based on density functional theory calculations (B3LYP/LanL2DZ) using Spartan '18 (Wavefunction, Inc.) and the

ionic radii were tentatively calculated assuming spheres of the same volumes as the respective ions [6].

4.2. Synthesis

Salt **1** was synthesized as follows. Under a nitrogen atmosphere, SO_2Cl_2 (0.025 mL, 0.31 mmol) was added dropwise to a dichloromethane solution (0.5 mL) of [FeCp*$_2$] (48 mg, 0.15 mmol) and stirred for 15 min. The solvent was then evaporated under reduced pressure and vacuum dried. The resulting dark green solid of [FeCp*$_2$]Cl was dissolved in water (0.5 mL), to which an aqueous solution (0.2 mL) of K[CH_2BrBF_3] (54 mg, 0.27 mmol) was added and stirred for 15 min. The resulting precipitate was collected by filtration and washed with ether, followed by drying under vacuum to obtain the desired product as a dark green solid. Recrystallization by slow cooling (−40 °C) of an ether-dichloromethane solution of the solid afforded dark green block crystals of **1** (31.5 mg, yield 43%). Anal. Calcd. for $C_{21}H_{32}F_3BBrFe$: C, 51.68; H, 6.65; N, 0.00. Found: C, 51.88; H, 7.05; N, 0.00. IR (cm^{-1}): 2949, 1474, 1424, 1381, 1186, 1124, 1104, 1081, 1043, 1025, 996, 968, 954, 742, 722, 619, 593, 531.

Salt **2** was synthesized using the same method but with [Fe($C_5Me_4H)_2$] to afford dark green block crystals (yield 30%). Anal. Calcd. for $C_{19}H_{28}F_3BBrFe$: C, 49.61; H, 6.14; N, 0.00. Found: C, 49.28; H, 6.30; N, 0.01. IR (cm^{-1}): 2918, 1454, 1424, 1384, 1336, 1179, 1101, 1044, 1026, 997, 974, 961, 747, 725, 620, 571, 559, 532.

Salt **3** was synthesized as follows. Under a nitrogen atmosphere, K[CH_2BrBF_3] (98 mg, 0.49 mmol) was added to an aqueous solution (0.4 mL) of [FeCp$_2$]Cl (72 mg, 0.34 mmol) and stirred for 30 min. The solution was extracted with dichloromethane (1 mL × 4) and diethyl ether was slowly diffused into the solution at −6 °C for 1 day to afford the dark blue needle crystals of **3** (20.2 mg, yield 17%). Anal. Calcd. for $C_{11}H_{12}F_3BrBFe$: C, 37.99; H, 3.48; N, 0.00. Found: C, 38.86; H, 3.54; N, 0.03. IR (cm^{-1}): 3105, 1418, 1229, 1192, 976, 853, 757, 741, 722, 683, 626, 572, 557, 544, 540, 532.

4.3. X-ray crystal structure determination

Single crystals of **1** and **3** suitable for X-ray structural analysis were prepared by slow cooling of the acetone-ether solution of **1** and diffusion of ether into a dichloromethane solution of **3**. A Bruker APEX II Ultra (Mo*K*α radiation) diffractometer was used for data collection and SHELXL [14] was used for the analysis. The crystallographic parameters are listed in Table 2.

Table 2. Crystallographic parameters.

	1	**3**
Empirical formula	$C_{21}H_{32}BBrF_3Fe$	$C_{11}H_{12}BBrF_3Fe$
Formula weight	488.03	347.78
Crystal system	Triclinic	Orthorhombic
Space group	*P*-1	*Pmmn*
a [Å]	8.3605(6)	18.300(3)
b [Å]	10.2394(8)	18.660(3)
c [Å]	13.1044(10)	7.0491(13)
α [°]	88.7470(10)	90
β [°]	82.1300(10)	90
γ [°]	85.7450(10)	90
V [Å^3]	1108.11(14)	2407.1(8)
Z	2	8
ρ_{calcd} [g cm^{-3}]	1.463	1.919
F(000)	502	1368
Temperature [K]	223	100
Reflns collected	5351	11768
Independent reflns	3828	2398
Parameters	254	199
R(int)	0.0167	0.0239
$R_1{}^a$, $R_w{}^b$ ($I > 2\sigma$)	0.0382, 0.1051	0.0646, 0.1787
$R_1{}^a$, $R_w{}^b$ (all data)	0.0396, 0.1064	0.0650, 0.1789
Goodness of fit	1.080	0.826
$\Delta\rho_{max,min}$ [e Å^{-3}]	0.604, –0.972	1.770, –2.090

$^aR_1 = \Sigma||F_o| - |F_c|| / \Sigma|F_o|$. $^bR_w = [\Sigma w (F_o^2 - F_c^2)^2 / \Sigma w (F_o^2)^2]^{1/2}$

Acknowledgements

We are grateful to Dr. Takahiro Sakurai and Prof. Hitoshi Ohta (Kobe University) for their help with the SQUID measurements. This work was financially supported by KAKENHI (grant number

16H04132) from the Japan Society for the Promotion of Science (JSPS).

Appendix A. Supplementary material

CCDC 1899037 (**1**) and 1899038 (**3**) contain the supplementary crystallographic data for this paper. These data can be obtained free of charge from the Cambridge Crystallographic Data Center via www.ccdc.cam.ac.uk/data_request/cif. Supplementary data to this article can be found online at -

References

[1] a) D.R. MacFarlane, J. Huang, M. Forsyth, Nature 402 (1999) 792–794;

b) J.M. Pringle, Phys. Chem. Chem. Phys. 15 (2013) 1339–1351;

c) K. Matsumoto, U. Harinaga, R. Tanaka, A. Koyama, R. Hagiwara, K. Tsunashima, Phys. Chem. Chem. Phys. 16 (2014) 23616–23626;

d) Y. Abu-Lebdeh, P.-J. Alarco, M. Armand, Angew. Chem. Int. Ed. 42 (2003) 4499–4501; Angew. Chem. 115 (2003) 4637–4639;

e) Z.B. Zhou, H. Matsumoto, Electrochem. Commun. 9 (2007) 1017–1022;

f) J. Luo, A.H. Jensen, N.R. Brooks, J. Sniekers, M. Knipper, D. Aili, Q. Li, B. Vanroy, M. Webbenhorst, F. Yan, L.V. Meervelt, Z. Shao, J. Fang, Z.-H. Luo, D.E. De Vos, K. Binnemans, J. Fransaer, Energy Environ. Sci. 8 (2015) 1276–1291;

g) M. Lee, U.H. Choi, S. Wi, C. Slebodnick, R.H. Colby, H.W. Gibson, J. Mater. Chem. 21 (2011) 12280–12287.

h) T. Hayasaki 1 , S. Hirakawa, H. Honda, Bull. Chem. Soc. Japan 86 (2013) 993–1001.

[2] a) J. Timmermans, J. Phys. Chem. Solids 18 (1961) 1–8;

b) J. Sherwood, The Plastically Crystalline State: Orientationally Disordered Crystals, Wiley, Chichester, 1979.

[3] a) R.J. Webb, M.D. Lowery, Y. Shiomi, M. Sorai, R.J. Wittebort, D.N. Hendrickson, Inorg. Chem. 31 (1992) 5211–5219;

b) D. Braga, F. Paganelli, E. Tagliavini, S. Casolari, G. Cojazzi F. Grepioni, Organometallics 18 (1999) 4191–4196;

c) H. Schottenberger, K. Wurst, U.J. Griesser, R.K.R. Jetti, G. Laus, R.H. Herber, I. Nowik, J. Am. Chem. Soc. 127 (2005) 6795–6801.

[4] T. Mochida, Y. Funasako, M. Ishida, S. Saruta, T. Kosone, T. Kitazawa, Chem. Eur. J. 22 (2016) 15725–15732.

[5] T. Mochida, M. Ishida, T. Tominaga, K. Takahashi, T. Sakurai, H. Ohta, Phys. Chem. Chem. Phys. 20 (2018) 3019–3028.

[6] H. Kimata, T. Mochida, Cryst. Growth Des. 18 (2018) 7562–7569.

[7] H. Kimata, T. Sakurai, H. Ohta, T. Mochida, ChemistrySelect 4 (2019) 1410–1415.

[8] I. de Pedro, A. García-Saiz, J. A. González, I. Ruiz de Larramendi, T. Rojo, C. Afonso, S. Simeonov, J. C. Waerenborgh, J. A. Blanco, B. Ramajo J. Rodríguez, Phys. Chem. Chem. Phys. 15 (2013) 12724–12733.

[9] P. Atkins, T. Overton, J. Rourke, M. Weller, F. Armstrong, Shriver and Atkins' Inorganic Chemistry, Oxford University Press, Oxford, 2010.

[10] D.N. Hendrickson, Y.S. Sohn, H.B. Gray, Inorg. Chem. 10 (1971) 1559–1563.

[11] J. Harada, T. Shimojo, H. Oyamaguchi, H. Hasegawa, Y. Takahashi, K. Satomi, Y. Suzuki, J. Kawamata, T. Inabe, Nat. Chem. 11 (2016) 1–7.

[12] Y. Funasako, T. Mochida, T. Inagaki, T. Sakurai, H. Ohta, K. Furukara, T. Nakamura, Chem. Commun. 47 (2011) 4475–4477.

[13] J.J. Adams, N. Arulsamy, B.P. Sullivan, D.M. Roddick, A. Neuberger, R.H. Schmehv, Inorg. Chem. 54 (2015) 11136–11149.

[14] G. M. Sheldrick, Acta Crystallogr. A64 (2008) 112–122.

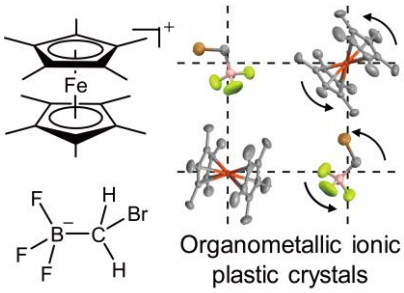

Highlights

$[Fe(L)_2][CH_2BrBF_3]$ (L = C_5Me_5, C_5Me_4H, C_5H_5) exhibited an ionic plastic phase

$[Fe(C_5Me_4H)_2][CH_2BrBF_3]$ exhibited a plastic phase at ambient temperature.

The phase behaviors of the CH_2BrBF_3 and CF_3BF_3 salts differed significantly.